Available online at www.sciencedirect.com
ScienceDirect
Ceramics International 34 (2008) 1425–1429
CERAMICS INTERNATIONAL
www.elsevier.com/locate/ceramint

Two-step method fabricating high nonlinearity ZnVSb based varistors

Ming Zhao [a,b,*], Xiang Chun Liu [a], Wei Min Wang [a], Feng Gao [a], Chang Sheng Tian [a]

[a] School of Material Science and Engineering, Northwestern Polytechnical University, Xi'an, Shaanxi 710072, PR China
[b] School of Material-Metallurgy Science and Engineering, Inner Mongolia University of Science and Technology, Bao Tou, Inner Mongolia 014010, PR China

Received 31 July 2006; received in revised form 21 February 2007; accepted 28 March 2007
Available online 5 May 2007

Abstract

A two-step method was introduced to fabricate ZnO–V_2O_5–Sb_2O_3 (ZnVSb) based varistor at low temperatures, such as 900–950 °C. Sb_2O_3/V_2O_5 (V/Sb) precursor was first synthesized and then used to replace Sb_2O_3 as one of the main dopants. The effect of its concentration on the microstructure and electrical properties of the ZnVSb based ceramic was investigated at doping levels up to 1.5 mol%. The microstructural homogeneity of the ceramic was greatly improved by the addition of the precursor. With increasing V/Sb precursor, the average grain size decreased, while the nonlinearity of the as sintered ceramic was enhanced ($\alpha_{Max} = 89$). The ZnVSb ceramic is a promising material in the fabrication of multi-layered varistor, in which it could be co-sintered with pure Ag inner electrode.

Keywords: D. ZnO; E. Varistors; Ceramic; Precursor

1. Introduction

ZnO–V_2O_5 based varistor ceramic has been consistently studied because of its outstanding low temperature sintering capability and the potentiality of replacing ZnO–Bi_2O_3 based ceramic in the fabrication of multi-layered varistors, in which the ceramic can be co-sintered with pure Ag inner electrode [1,2]. However, heterogeneity of the granular structure contributes to nonuniform conduction in varistor ceramic, which may create hot spots and localized degradation of the material [3]. Such microstructural defects in ZnO–V_2O_5 based varistor ceramic have been reported in several peer researches [1,2,4]. A recent research showed microstructural heterogeneity in ZnO–V_2O_5 based ceramic can be alleviated by adding 2 mol% of Sb_2O_3 [5]. However, the sintering temperature of the ceramic was increased to 1200 °C because of the hindering effect of Sb_2O_3 amorphous film and zinc antimony spinel particles on the grain growth of the ceramic during sintering process [5]. Similar phenomenon was also observed in ZnO–Sb_2O_3 ceramic system [6]. According to this report, the hindering effect of Sb_2O_3 amorphous film could be eliminated if Sb_2O_3 had been pre-heated with Bi_2O_3. Therefore, similar approach is a promising way to synthesis ZnO–V_2O_5–Sb_2O_3 (ZnVSb) based varistor ceramic at relatively low temperatures, such as 900–950 °C.

In our work, an extra step of pre-heating Sb_2O_3 with V_2O_5 was introduced to fabricate ZnVSb based varistor ceramic. The effects of the Sb_2O_3/V_2O_5 (V/Sb) precursor content on the microstructure and electrical properties of the ceramic were studied according to XRD, SEM and electrical property measurements.

2. Experimental procedure

2.1. Sample preparation

Analytical grade powdered materials were used to fabricate V/Sb precursor and ceramic specimens by conventional methods. The precursor used in the present study was synthesized by heating a mixture of Sb_2O_3 and V_2O_5 with a molar ratio of 4:1 at 650 °C for 1 h. X-ray powder diffraction (XRPD) test result, as shown in Fig. 1, shows it is actually a mixture of Sb_2O_4 (JCPDS:80-0231) and $SbVO_4$ (JCPDS:88-0278) with a molar ratio of 3:2. The precursor was then used to replace all Sb_2O_3 in the ceramic of following compositions: ZnO + 0.5 mol% V_2O_5 + 0.3% Co_2O_3 + 0.2% Mn_3O_4 + 0.01%

* Corresponding author at: School of Material Science and Engineering, Northwestern Polytechnical University, Xi'an, Shaanxi 710072, PR China.
E-mail address: philipzo@yahoo.com (M. Zhao).

0272-8842/$34.00
doi:10.1016/j.ceramint.2007.03.027

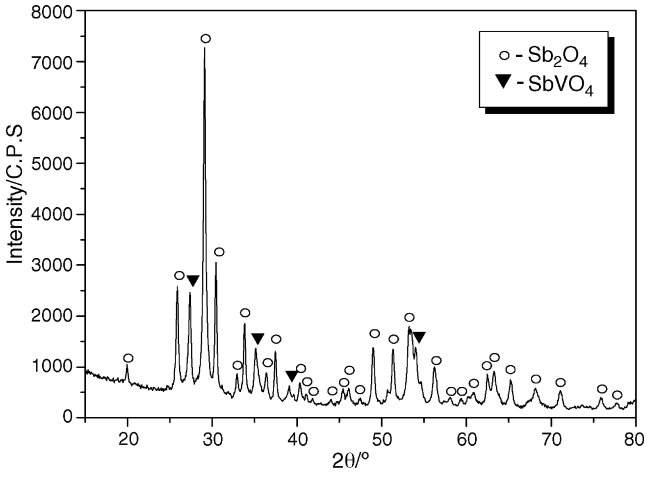

Fig. 1. The XRD pattern of as synthesized V/Sb precursor.

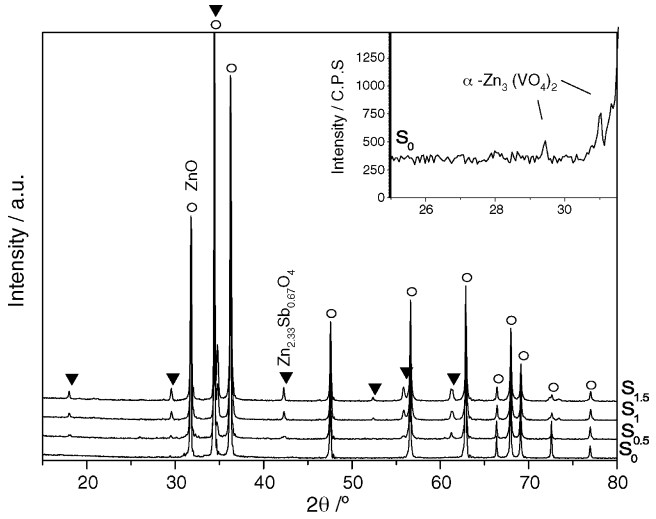

Fig. 2. The XRD patterns of the ZnVSb based varistor ceramics, showing the phase constituent variations of the ZnVSb based varistor ceramics with the increase of V/Sb precursor concentration.

$Nb_2O_5 + x\%$ Sb_2O_3. Specimens of these four compositions named as S_0, $S_{0.5}$, S_1, $S_{1.5}$ were made with $x = 0$, 0.5, 1, 1.5, respectively. At the same time, the amount of V_2O_5 within each composition was also reduced accordingly. Starting materials of four formulations was mixed, respectively, by ball milling with zirconia balls and absolute alcohol in a polypropylene container for 24 h. After drying, the mixtures were pressed into pellets of Ø 12 mm × 1.5 mm under uniaxial pressure of 130 MPa. The pellets were sintered at temperatures of 900, 950, 1000 and 1050 °C in air for 4 h with heating rates of 5 °C/min. After sintering, the furnace was turned off, allowing the sintered pellets to be cooled down naturally within the furnace.

2.2. Method of characterization

The crystalline phases of the precursor and as sintered ceramic specimen were identified on a X-ray diffractometer (Model Xpert, Netherlands) using Cu $K\alpha_1$ radiation ($\lambda = 0.1541$ nm). Microstructures of polished and etched specimens were examined by SEM (JEOL JSM 5800) equipped with energy dispersive X-ray analysis (EDX). Average ZnO grain size was measured by the intercept method as described by Mendelson [7]. Density of the ceramic specimen was decided by dividing the mass by volume, and the relative density ρ_r was calculated with the respect to the theoretical density of zinc oxide varistor ceramic (5.675 g/cm^3) [1].

Before the electrical measurement, the samples were lapped on both sides to ensure flat and paralleled surfaces, and then silver electrodes were fired on both sides of the sample to form ohmic contacts. Current–voltage (I–V) characteristics were determined at room temperature using a variable DC power supply. The nonlinearity exponent (α) of as tested sample was examined for a current density ranges from 1.0 to 10 mA/cm^2. The leak current density (I_L) was tested at a voltage of 0.83 $V_{1\ mA}$. The capacitance–voltage (C–V) characteristics were determined using the same methods as described elsewhere [8,9].

3. Results and discussions

3.1. X-ray powder diffraction

XRPD patterns for samples sintered at 1000 °C are given in Fig. 2. ZnO is the predominant phase of all samples. $Zn_3(VO_4)_2$ (JCPDS No.34-0378) was detected as the secondary phase for S_0 sample. The appearance of the $Zn_3(VO_4)_2$ phase is consistent with earlier reports of V_2O_5-doped ZnO ceramics sintered at 900 °C [1,2]. For $S_{0.5}$, S_1 and $S_{1.5}$ samples, only $Zn_{2.33}Sb_{0.67}O_4$ (JCPDS No.15-0687) spinel was detected as the secondary phase. The presence of $Zn_3(VO_4)_2$ or other forms of zinc vanadates within these samples could not be confirmed by present XRPD analysis. The reason can be ascribed to the scarce amount of V dopant and also the fact that the main peaks of $Zn_3(VO_4)_2$ have already been overlapped by those of spinel and ZnO [5]. Further tests, such as TEM, are needed to identify the phase constituents of these three samples. Moreover, a gradual intensity increase of the spinel concentration was also observed within latter three ceramic specimens, indicating the enhanced spinel formations by increasing V/Sb precursor concentration.

3.2. Microstructural observation

The SEM images of the ceramic specimens sintered at 950 °C for 4 h are shown in Fig. 3. In S_0 sample, some abnormal large grains can be easily observed, indicating a heterogeneous feature of the microstructure. This is in accordance with the previous studies on ZnO–V_2O_5 based varistor ceramic [1,2,4,5]. In contrast, $S_{0.5}$, S_1 and $S_{1.5}$ samples mainly consist of equiaxial ZnO grains of similar sizes, indicating the microstructural homogeneity was improved by V/Sb precursor. Fig. 3 also shows the average grain size decreases with the increase of the V/Sb precursor concentration. Several spinel particles on the grain boundaries, as well as within the ZnO grains, can be seen in a high magnification SEM image shown in Fig. 4. These spinel particles are known to have hindering effect on ZnO grain growth by

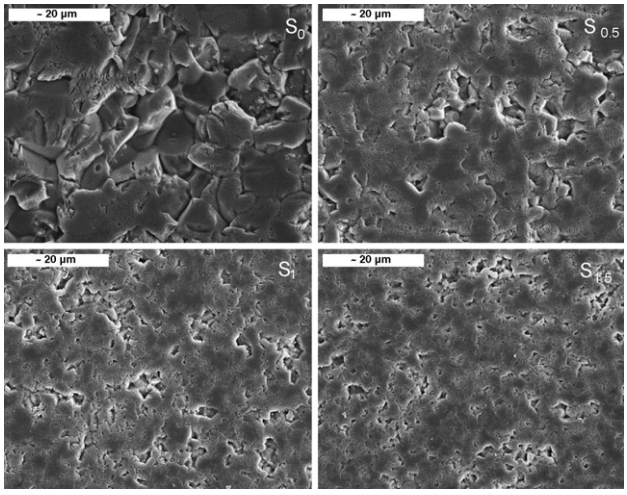

Fig. 3. Microstructure evolution of ZnVSb based ceramic sintered at 950 °C as a function of V/Sb precursor concentration.

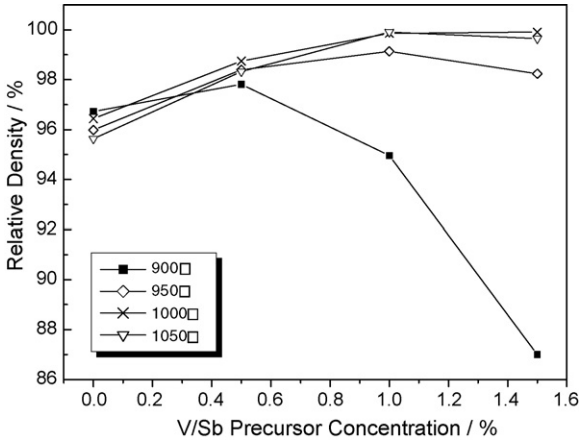

Fig. 5. Variations of the relative density of ZnVSb ceramics with the increases of V/Sb precursor concentration and sintering temperature. The samples were sintered for 4 h at 900, 950, 1000 and 1050 °C, respectively.

pinning the movement of the grain boundaries during the sintering process [10]. With spinel particles scattering within the grain boundary areas, the abnormal and normal grain growths of ZnO grains were both suppressed. Consequently, microstructure homogeneity of the precursor doped samples was greatly improved and the grain size of $S_{0.5}$, S_1 and $S_{1.5}$ samples decreased with the increase of V/Sb precursor concentration.

3.3. Density

Fig. 5 shows the effect of V/Sb precursor concentration on relative density of the samples sintered at four different temperatures. The relative density of all samples sintered at and above 950 °C is more than 95%. This indicates the samples have been well sintered. Similar high relative density was also achieved by S_0 and $S_{0.5}$ samples sintered at 900 °C. These results are consistent with the low temperature sintering capability of ZnO–V_2O_5 based ceramic at 900–950 °C [1,2,4,5,11]. Therefore, the sintering process of V/Sb precursor doped ZnVSb ceramic also has the same feature of liquid phase assisting sintering. With the further increase of V/Sb precursor concentration, the relative density of S_1 and $S_{1.5}$ samples sintered at 900 °C continually decreases to lower values. The main reason can be ascribed to the hindering effect of spinel particles on the grain growth of ZnVSb based ceramic.

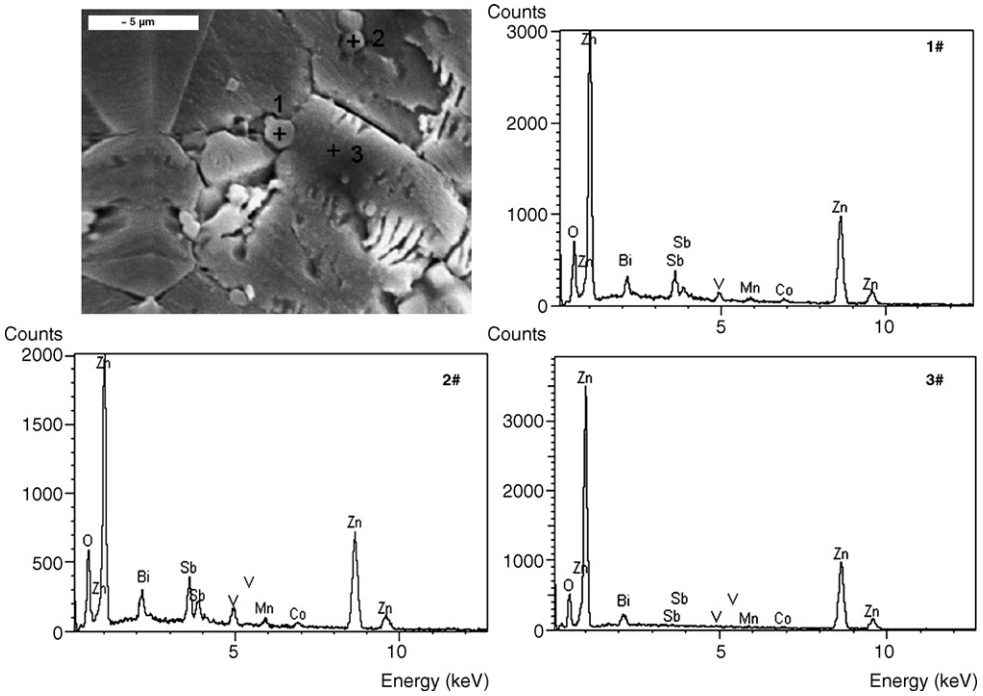

Fig. 4. A high magnification SEM photo of 1050 °C sintered $S_{0.5}$ sample, showing the distributions of the spinel particles at grain boundaries and within the ZnO grain; and X ray spectra of spinel particle at the grain boundary (1#), within the ZnO grain (2#) and that of ZnO grain (3#), showing the dopant elements distribution within the microstructure of ZnVSb based varistor ceramic.

Table 1
The relative densities of the $S^*_{0.5}$ sintered at 900 and 950 °C

Sample	Sb_2O_3 (mol%)	Sintering temp. (°C)	Time (h)	ρ_r (%)
$S^*_{0.5}$	0.5	900	4	90
$S^*_{0.5}$	0.5	950	4	95

However, the above result contradicts with the poor densification characteristic of 2 mol% Sb_2O_3 doped ZnO–V_2O_5 based varistor [5]. For comparison, a sample was prepared using Sb_2O_3 without the pre-heating treatment. The composition of the sample was the same as that of $S_{0.5}$ and designated as $S^*_{0.5}$. The sintering results are shown in Table 1.

This sample was not fully sintered at 900 °C. As the temperature was increased to 950 °C, a relative density of 98% was achieved, showing well sintering. The result of this comparison sintering test is consistent with a detailed study of the effect of Sb_2O_3 on the densification of ZnO ceramic [6]. According to this report, Sb_2O_3 starts to evaporate at 500 °C and re-coagulate on the surfaces of growing ZnO grains to form a thin amorphous film. The densification of the ceramic cannot start until the amorphous Sb_2O_3 film is eliminated by the formation of crystalline $Zn_7Sb_2O_{12}$ spinel particle at 900 °C. This explains why $S^*_{0.5}$ sample could not be well sintered at 900 °C. In other words, the prevention of Sb_2O_3 amorphous film formation from pre-heating Sb_2O_3 with V_2O_5 is highly feasible to be the main reason to the low temperature sintering of the ZnVSb based ceramic. This assumption is also supported by the facts that no Sb_2O_3 was detected from the V/Sb precursor (Fig. 1) and Sb_2O_4 has been confirmed having no hindering effect on the grain growth of ZnO ceramic by means of forming the same type of amorphous film [6].

3.4. Electrical characteristics

The electrical properties of ZnO based varistor ceramic can be presented by its *I–V* and *C–V* characteristics. The values of electrical parameters derived from *I–V* and *C–V* tests of samples sintered at 950 °C have been summarized in Table 2. The *I–V* test results show that both nonlinearity exponent α and breakdown voltage V_B increase dramatically, from 24 and 162 V/mm in S_0 sample to 89 and 1277 V/mm in $S_{1.5}$ sample, respectively, while the leak current density J_L remains rather constant. The *C–V* measurement results show constant increases in both values of barrier height Φ_B and depletion layer thickness w, from 0.68 eV and 1.76×10^{-8} m in S_0 sample to 4.32 eV and 9.259×10^{-8} m in $S_{1.5}$ sample. On the contrary, donor density N_d generally decreases from $20.8 \times 10^{23}\ m^{-3}$ in S_0 ceramic, to $4.73 \times 10^{23}\ m^{-3}$ in $S_{1.5}$ ceramic. Moreover, the value of N_S first decreases with the addition of the precursor, from $3.635 \times 10^{16}\ m^{-2}$ in S_0 sample to $3.217 \times 10^{16}\ m^{-2}$ in $S_{0.5}$ sample, then increases slightly with the further increase of the precursor concentration.

It is generally accepted that the nonohmic characteristic of ZnO based varistor ceramic depends on the dopant element segregations on the grain boundary [12]. EDS analysis shown in Fig. 4 (spectra 1#, 2# and 3#) reveals that the concentrations of V, Mn and Co within spinel particles are higher than those within ZnO grain. XRPD showed the spinel particle formation within the ZnVSb ceramics was enhanced by increasing addition of V/Sb precursor. And antimony ions have been reported having a low solid solubility within the ZnO grains [13]. Accordingly, while the concentrations of V, Mn and Co within the ZnVSb based ceramic were maintained stable, the value of N_d would generally decrease with the addition of V/Sb precursor because of more absorption of above mentioned donor elements in spinel particles. Moreover, the spinel induced dopant elements redistribution may also account for the observed gradual improvements of Φ_B and w of the V/Sb precursor doped ceramics. This may be ascribed to more dopant elements, such as Mn and Co, were absorbed within the spinel with the increase of the V/Sb precursor concentration within ZnVSb based ceramic. When the samples were cooled down from the soaking temperature, part of those already absorbed dopant elements was released by spinel particles due to the decrease of solid solubility. Most of them would segregate at grain boundary, as their solid solubility within the ZnO grain also decreased during cooling. Transition metal elements, such as Mn or Co, are known to be the most effective nonlinearity enhancing elements within ZnO varistor ceramic, because ions of these two elements contribute to the interface state and barrier formations of on the grain boundaries [12]. Consequently, the values of w and Φ_B of the ZnVSb ceramics were increased with more addition of V/Sb precursor, and the electrical nonlinearity of the ceramics was improved.

Previous studies showed that the spinel particle induced stress state could serve as another driving force of the segregations of interstitial ions, such as $Zn_i^{\prime}$ and $Zn_i^{\prime\prime}$, at grain boundary [14]. Analogously, this stress may also contribute to the observed dopant element segregations at grain boundaries.

Table 2
The electrical characteristic parameters of the ZnVSb based varistor ceramics

Sample	Average grain size (μm)	ρ_r (%)	I_L (μA/cm^2)	V_B (V/mm)	α	N_d ($\times 10^{23}\ m^{-3}$)	Φ_B (eV)	w ($\times 10^{-8}$ m)	N_s ($\times 10^{16}\ m^{-2}$)
$S_{0.5}$[a]	2.50	98.0	76	900	70	11.1	1.24	3.238	3.599
S_0	6.88	95.99	85.21	162	24	20.8	0.68	1.76	3.653
$S_{0.5}$	3.31	98.4	60	541	56	9.21	1.2	3.492	3.217
S_1	2.65	99.0	42	1138	74	9.51	2.12	4.579	4.355
$S_{1.5}$	2.69	98.2	>200	1277	89	4.73	4.32	9.259	4.377
$S^*_{0.5}$	2.60	98.3	53	1268	84	5.57	2.70	6.75	3.757

[a] Ceramic sintered at 900 °C.

Further electrical measurement showed that the sample $S_{0.5}$ sintered at 900 °C also exhibited an outstanding current–voltage nonlinearity ($\alpha = 70$) and a breakdown voltage of 900 V/mm. Both values are higher than those of the $S_{0.5}$ ceramic sintered at 950 °C. The reason can be attributed to the deterioration of the dopant element segregations at the grain boundary at a higher temperature.

4. Conclusions

V_2O_5/Sb_2O_3 precursor was prepared by a pre-heating treatment of Sb_2O_3 with V_2O_5 and then used as one of main dopants to fabricate ZnVSb based varistor ceramics. By this approach, the hindering effect of Sb_2O_3 amorphous film on the growth of ZnO grains was avoided. Therefore, the ceramic could be well sintered at 900–950 °C. Other than main phase ZnO, $Zn_{2.33}Sb_{0.67}O_4$ spinel was the predominant secondary phase within the precursor doped ZnVSb based ceramics, while $Zn_3(VO_4)_2$ was detected as the only secondary phase of the ceramic without the precursor. The spinel formation was progressively enhanced by increasing the concentration of the precursor, which resulted in the gradual decrease of average grain size and the microstructure homogenization of the ceramics. The dopant segregations at grain boundary were also enhanced at the same time. It contributes mainly to the observed high nonlinearity ($\alpha_{max} = 89$) of the ceramic. The features of low temperature sintering, relatively homogenous microstructure and high nonlinearity of the ZnVSb based ceramic make it a promising material in the fabrication of multi-layered chip varistor using pure Ag inner electrode.

Acknowledgements

Partial financial support by National Nature Science Council of P.R.O.C through grant No. 60501015 is gratefully acknowledged by the authors. We would also like to thank Yan ling Ai of NWPU, senior engineer Ke Yong Wang of China Contemporary Chemistry Research Institute for their help in XRD and SEM analysis. Sincere thanks are also extended to Shameel Farhan, employee of Pakistan government, for his help with the revising of this paper.

References

[1] J.K. Tsai, T.B. Wu, Microstructure and nonohmic properties of ZnO–V_2O_5 ceramic, Jpn. J. Appl. Phys. 34 (1995) 6452–6457.
[2] H.H. Hng, P.L. Chan, Microstructure and current–voltage characteristics of ZnO–V_2O_5–MnO_2 varistor system, Ceram. Int. 30 (2004) 1647–1653.
[3] F. Perrot, An efficient way to characterize the performance of metal oxide varistors, High Voltage Engineering Symposium, Conference Publication, No. 467, ©IEE, 1999, pp. 22–27.
[4] H.H. Hng, L. Halim, Grain growth in sintered ZnO–1 mol% V_2O_5 ceramic, Mater. Lett. 57 (2003) 1411–1416.
[5] H.H. Hng, K.M. Knowles, Microstructure and current–voltage characteristics of multicomponent vanadium-doped zinc oxide varistor, J. Am. Ceram. Soc. 83 (10) (2000) 2455–2462.
[6] J. Kim, T. Kimura, T. Yamaguchi, Sintering of Sb_2O_3-doped ZnO, J. Mater. Sci. 24 (1989) 213–219.
[7] M.I. Mendelson, Average grain size in polycrystalline ceramic, J. Am. Ceram. Soc. 52 (8) (1969) 443–446.
[8] K. Mukae, K. Tsuda, I. Nagasawa, Capacitance-vs-voltage characteristics of ZnO varistors, J. Appl. Phys. 50 (6) (1979) 4475–4476.
[9] S. Bernik, N. Daneu, Characteristics of SnO_2-doped ZnO-based varistor ceramic, J. Eur. Ceram. Soc. 21 (2001) 1879–1882.
[10] J. Wong, Microstructure and phase transformation in highly non-ohmic metal oxide varistor ceramic, J. Appl. Phys. 46 (4) (1975) 1653–1659.
[11] H.H. Hng, P.L. Chan, Microstructure and current–voltage characteristics of ZnO–V_2O_5–MnO_2 varistor system [J], Ceram. Int. 30 (2004) 1647–1653.
[12] T.K. Gupta, The application of zinc oxide varistor, J. Am. Ceram. Soc. 73 (7) (1990) 1817–1840.
[13] J.M. Carlsson, B. Hellsing, H.S. Domingos, Electronic properties of a grain boundary in Sb-doped ZnO, J. Phys. Condens. Matter 13 (2001) 9937–9943.
[14] C.Y. Shen, Y.C. Chen, L. Wu, The effect of antimony oxide on the electrical properties and stability of ZnO varistors, Jpn. J. Appl. Phys. 32 (1993) 1147–1153.